Mechanical Systems and Signal Processing 23 (2009) 2648–2657

Contents lists available at ScienceDirect

Mechanical Systems and Signal Processing

journal homepage: www.elsevier.com/locate/jnlabr/ymssp

Hilbert versus Concordia transform for three-phase machine stator current time-frequency monitoring

Baptiste Trajin [a,b,*], Marie Chabert [c], Jérémi Regnier [a,b], Jean Faucher [a,b]

[a] Université de Toulouse; INP, UPS; LAPLACE; ENSEEIHT, 2 Rue C. Camichel - BP 7122, F-31071 Toulouse Cedex 7, France
[b] CNRS; LAPLACE, 2 Rue C. Camichel - BP 7122, F-31071 Toulouse Cedex 7, France
[c] Université de Toulouse; INPT/ENSEEIHT - IRIT, 2 Rue C. Camichel - BP 7122, F-31071 Toulouse Cedex 7, France

ARTICLE INFO

Article history:
Received 25 March 2009
Received in revised form
18 May 2009
Accepted 26 May 2009
Available online 6 June 2009

Keywords:
Analytic signal
Hilbert transform
Bedrosian theorem
Fast modulations
Concordia transform
Space vector
Wigner distribution
Induction machine
Stator current analysis

ABSTRACT

This paper deals with mechanical fault diagnosis in three-phase induction machines from stator current measurements. According to machine models, mechanical faults lead to amplitude and/or phase modulations of the measured stator current with possibly time varying carrier frequency. The modulation diagnosis requires a univocal definition of the instantaneous phase and amplitude. This is performed by associating a complex signal to the real measured one. For a convenient separate modulation diagnosis, the complex signal instantaneous phase and amplitude are expected to carry, respectively, information about the phase and amplitude modulations. The complex signal is classically obtained through the Hilbert transform. Under Bedrosian conditions, the so-called analytic signal allows a separate modulation diagnosis. However, mechanical faults may also produce fast modulations violating the Bedrosian conditions. This study proposes an alternative complex signal representation which takes advantage of the three stator current measurements available in a three-phase machine. From two stator current measurements, the Concordia transform builds a complex vector, the so-called space vector, which unconditionally allows separate modulation diagnosis. This paper applies and compares the Hilbert and Concordia transforms, theoretically and in case of simulated and experimental signals with various modulation frequency ranges.

1. Introduction

Monitoring techniques are intensively investigated to increase the reliability and safety of industrial systems using induction motors. Mechanical faults such as eccentricity and load torque oscillations have been shown to produce, respectively, amplitude modulation (AM) and phase modulation (PM) of the stator current [1]. In steady state i.e. fixed carrier frequency, the diagnosis is traditionally based on the stator current spectral analysis [2]. However, the Wigner distribution (WD) allows to detect and classify the faults through their time-frequency signatures in steady state operation as well as at variable speed, and thus time-varying carrier frequency [3,4]. Through spectral or time-frequency analysis, the study of AM and PM requires a rigorous definition of instantaneous amplitude (IA) and instantaneous phase (IP). For that purpose, a complex signal must be associated to the real measured signal. For a convenient diagnosis, the IA and IP are expected to carry information about AM and PM, respectively. The complex signal is classically obtained through the Hilbert transform (HT) of the real measured signal [5–8]. Under Bedrosian conditions related to modulation and carrier

* Corresponding author at: Université de Toulouse; INP, UPS; LAPLACE; ENSEEIHT, 2 Rue C. Camichel - BP 7122, F-31071 Toulouse Cedex 7, France. Tel.: +33 (0)5 61 58 83 61; fax: +33 (0)5 61 63 88 75.
E-mail addresses: baptiste.trajin@laplace.univ-tlse.fr (B. Trajin), marie.chabert@enseeiht.fr (M. Chabert), jeremi.regnier@laplace.univ-tlse.fr (J. Regnier), jean.faucher@laplace.univ-tlse.fr (J. Faucher).

0888-3270/$ - see front matter © 2009 Elsevier Ltd. All rights reserved.
doi:10.1016/j.ymssp.2009.05.015

frequencies [9], the so-called analytic signal allows a separate modulation diagnosis. However, several mechanical faults, such as bearing or gear box faults, induce modulation frequencies which violate the Bedrosian conditions [10]. The spectral or time-frequency signature can thus be misleading. Signals violating (respectively, respecting) the Bedrosian theorem conditions are defined as fast (respectively, slow) modulated signals.

The Concordia transform (CT) is often used in electrical engineering for control purposes [11,12] and in electrical or mechanical diagnosis to detect static converter defects [13], unbalanced electrical systems [14], machine stator electric defects [15,16], mechanical eccentricity [17] or bearing defects [18,19]. The main purpose of the CT is to reduce the number of variables describing the three-phase machine: this transform builds a complex variable from three real measurements [20]. This paper proposes the CT as an alternative to the HT to built a complex vector, in the case of three-phase machines. Then, a time-frequency analysis through the WD can be performed, even when the Bedrosian theorem conditions are violated. Section 2 presents the stator current model in case of two elementary mechanical faults: dynamic eccentricity and load torque oscillations. Section 3 recalls the HT, the Bedrosian theorem limitations and the CT. Section 4 compares the Hilbert analytic signal and Concordia space vector IA and IP for various modulation frequency ranges using simulated and experimental stator currents. HT and CT are also compared in terms of computing complexity. Finally, Section 5 studies time-frequency diagnosis and compares the AM and PM time-frequency signatures through WD via HT and CT.

2. Stator current model under mechanical faults

In three-phase machines, three current measurements with a phase separation of one-third cycle ($2\pi/3$ rad) are available. Assuming a first harmonic model, they can be written in the simple form:

$$i_k(t) = a(t)\cos(\psi(t) - \phi_k), \quad k = 1,2,3 \quad \text{with} \quad \phi_k = (k-1)\frac{2\pi}{3} \tag{1}$$

Using a first harmonic approach, the healthy machine is characterized by

$$\begin{cases} a(t) = I \\ \psi(t) = 2\pi f_s t + \psi_0 \end{cases}$$

where I denotes the stator current amplitude, f_s the machine supply frequency and ψ_0 is the initial phase. Mechanical faults lead to particular expressions of $a(t)$ and $\psi(t)$. Dynamic eccentricity and load torque oscillations are the main elementary mechanical faults [1]. They may be considered separately; however, a general default model that involves their combinations is proposed.

2.1. Amplitude modulation resulting from time varying airgap

The rotation of the rotor geometrical center around the geometrical stator center is called dynamic eccentricity. As a result, the point of minimum air-gap length is not stationary [21]. The time variation of the air-gap permeance causes an AM of the stator current [1,21,22] with carrier frequency f_s such as

$$\begin{cases} a(t) = I[1 + \alpha\cos(2\pi f_{am} t + \phi_{am})] \\ \psi(t) = 2\pi f_s t + \psi_0 \end{cases} \tag{2}$$

where α denotes the AM index, f_{am} the AM frequency and ϕ_{am} the AM initial phase. It can be noticed that the effects of dynamic eccentricity and time-varying air-gap length are similar. Moreover, the time-varying air-gap length caused by a geometrical deformation of the rotor may be such as $f_{am} > f_s$. In this case, this particular mechanical defect is said to induce fast AM on stator currents.

2.2. Phase modulation resulting from pure load torque oscillations

When submitted to periodic oscillations, the mechanical torque may be approximated by the first term of its Fourier series decomposition:

$$\Gamma_{load}(t) = \Gamma_0 + \Gamma_c\cos(2\pi f_{pm} t) \tag{3}$$

where Γ_c is the amplitude of the load torque oscillation and f_{pm} the oscillation frequency. The stator current may be approximated by a PM signal [1,3] such as

$$\begin{cases} a(t) = I \\ \psi(t) = 2\pi f_s t + \beta\sin(2\pi f_{pm} t + \phi_{pm}) + \psi_0 \end{cases} \tag{4}$$

where f_{pm} is the PM frequency, ϕ_{pm} is the PM phase, β is the PM index function of Γ_c, f_{pm} and f_s [1]. In case of bearing or gear box faults for instance, the load torque oscillation frequency is a high multiple of the rotating frequency leading to fast modulation of the measured current [10].

2.3. Mixed modulations resulting from general mechanical faults

More realistic fault models involve both time-varying air-gap length and load torque oscillations. As a consequence, the measured current general model may be written as follows:

$$\begin{cases} a(t) = I[1 + \alpha\cos(2\pi f_{am}t + \phi_{am})] \\ \psi(t) = 2\pi f_s t + \beta\sin(2\pi f_{pm}t + \phi_{pm}) + \psi_0 \end{cases}$$

Note that null AM and PM indexes ($\alpha = 0$ and $\beta = 0$) correspond to the stator current model in healthy conditions.

3. The need for a complex signal representation

The study of AM and/or PM requires the definition of the IA and IP. For a univocal definition, a complex signal has to be associated to the real observed signal [8]. Indeed, for a given real signal $x(t)$, there exists an infinite number of pairs $[A(t), \Psi(t)]$ such as $x(t) = A(t)\cos(\Psi(t))$. The definition of IA and IP requires the construction of a canonical pair i.e. in one-to-one correspondence with $x(t)$ [5–8].

3.1. Analytic signal via the Hilbert transform

The classical way to define the IA and IP is to associate a complex signal to the measured real signal $i(t)$ through the HT. Let $I(f)$ denote the Fourier transform (FT) of $i(t)$ along the frequency f. The associated analytic signal FT $I_{HT}(f)$ is given in [7]

$$I_{HT}(f) = I(f) + jH(f)I(f) \quad \text{with } H(f) = -j\,\text{sign}(f) \tag{5}$$

where

$$\text{sign}(f) = \begin{cases} +1 & \text{for } f > 0 \\ 0 & \text{for } f = 0 \\ -1 & \text{for } f < 0 \end{cases}$$

$H(f)$ is the Hilbert filter transfer function. Now let $i_{HT}(t) = a_{HT}(t)e^{j\psi_{HT}(t)}$ with $a_{HT}(t)$ non negative and $\psi_{HT}(t)$ defined modulo 2π. Then $a_{HT}(t)$ and $\psi_{HT}(t)$ are the IA and IP respectively [8]. It can be noticed that the HT leads to the cancelation of negative frequency components. When a modulation transfers significative components into the negative frequencies, the HT may yield misleading interpretations [5].

3.2. Bedrosian theorem conditions

One can consider a real stator current fundamental component $i(t) = i_1(t) = a(t)\cos(\psi(t))$. This signal can be considered as an AM and/or PM signal. The imaginary part of the analytic signal is expected to be the quadrature component of $i(t)$:

$$\Im(i_{HT}(t)) = h(t) * [a(t)\cos(\psi(t))] = a(t)\sin(\psi(t)) \tag{6}$$

where h denotes the impulse response of the Hilbert filter. In this case, $i_{HT}(t) = a(t)e^{j\psi(t)}$. The commutation between convolution and multiplication in (6) is only possible under the conditions of the Bedrosian theorem: the time-varying amplitude should have the characteristics of a low-pass signal whereas $\cos(\psi(t))$ should be a high-pass signal as depicted in Fig. 1, where c is an arbitrary constant [9]. Moreover, the bandwidth of $\cos(\psi(t))$ has to be relatively small.

In case of slow modulations, the HT provides $a_{HT}(t) = a(t)$ as the IA and $\psi_{HT}(t) = \psi(t)$ as the IP. Thus, the IA (respectively, IP) carries information about the AM (respectively, the PM). Note that the PM is preferentially studied through the instantaneous frequency (IF) defined by

$$IF(t) = \frac{1}{2\pi}\frac{d\psi_{HT}(t)}{dt}. \tag{7}$$

Finally, to obtain a complex signal, a component in quadrature with the real observed signal has to be derived. The HT allows to compute this component only for slow modulated signals. However, rotor geometrical deformations, bearing or

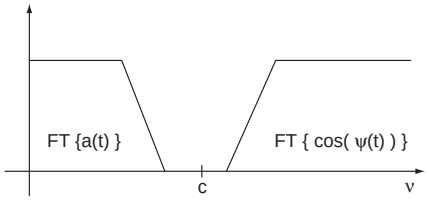

Fig. 1. Illustration of the Bedrosian theorem conditions.

gear box faults may produce fast modulations. In this case, a new strategy is proposed to build an appropriate complex signal by taking advantage of the three current measurements.

3.3. Concordia transform

In case of three-phase electrical machines, the three stator current measurements $i_1(t)$, $i_2(t)$ and $i_3(t)$ can be represented by a set of three coplanar vectors with a phase shift of $-2\pi/3$ rad (Fig. 2). The CT is a linear transform which defines an orthogonal basis i.e. two components in quadrature (u, v) from the three previous vectors [12,20]. This linear transform can be expressed with the normalized Clarke matrix:

$$\begin{pmatrix} u \\ v \end{pmatrix} = \frac{2}{3}\begin{pmatrix} 1 & -\frac{1}{2} & -\frac{1}{2} \\ 0 & \frac{\sqrt{3}}{2} & -\frac{\sqrt{3}}{2} \end{pmatrix}\begin{pmatrix} i_1 \\ i_2 \\ i_3 \end{pmatrix} \tag{8}$$

This study focuses on balanced systems satisfying the following condition $i_1(t) + i_2(t) + i_3(t) = 0, \ \forall t$. For such systems, the matrix in (8) is simplified in the Concordia matrix:

$$\begin{pmatrix} u \\ v \end{pmatrix} = \sqrt{\frac{2}{3}}\begin{pmatrix} \sqrt{\frac{3}{2}} & 0 \\ \frac{1}{\sqrt{2}} & \frac{2}{\sqrt{2}} \end{pmatrix}\begin{pmatrix} i_1 \\ i_2 \end{pmatrix} \tag{9}$$

A geometrical interpretation of this linear transform is displayed in Fig. 2. The Clarke matrix may be interpreted as a constant projection matrix. The complex space vector is defined by $i_{CT}(t) = u(t) + jv(t)$.

The CT is widely implemented in electrical drives for control purposes [11] and monitoring applications [15–19]. Generally, the Concordia space vector modulus is considered as the demodulated signal and allows to detect faulty operations. In these cases, the space vector argument is ignored. On the contrary, the proposed approach uses both the modulus and argument of the space vector to analyze the stator current IA and IF. Indeed, for the three current in the form (1), it can be easily shown from (9) that $i_{CT}(t) = a(t)e^{j\psi(t)}$ whatever the modulation and carrier frequencies.

4. Comparison of Hilbert analytic signal and Concordia space vector

4.1. Theoretical analysis

The frequency content of the IA and the IF obtained through HT and CT have been theoretically derived for the signal models (2) and (4) in case of slow and fast AM and PM. As an example, the case of fast PM is developed in Appendix A. Results are provided in Table 1.

The CT and HT provide the same complex signal for slow modulated signals. However, in case of fast modulations, extra harmonics appear in the IA and IF derived through HT. These extra harmonics may lead to a misleading diagnosis since pure AM and pure PM both appear as mixed AM/PM. Another key comparison criterion is the computational complexity. Indeed, in practical applications on sampled stator current signals, HT can be approximated by a finite impulse response filtering with relatively high order N [4]. It results in N multiplication/accumulation operations and in a delay of $N/2$ samples. On

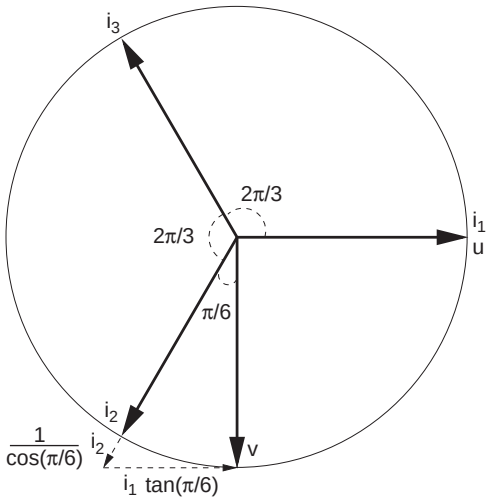

Fig. 2. Geometrical construction of the Concordia basis from the three current components.

Table 1
Harmonic frequencies in case of slow and fast AM and PM.

	AM		PM	
	Slow	Fast	Slow	Fast
HT				
IA	f_{am}	f_{am} $\lvert 2f_s - f_{am}\rvert$	None	f_{pm} $\lvert 2f_s - f_{pm}\rvert$
IF	None	f_{am} $\lvert 2f_s - f_{am}\rvert$	f_{pm}	f_{pm} $\lvert 2f_s - f_{pm}\rvert$
CT				
IA	f_{am}	f_{am}	None	None
IF	None	None	f_{pm}	f_{pm}

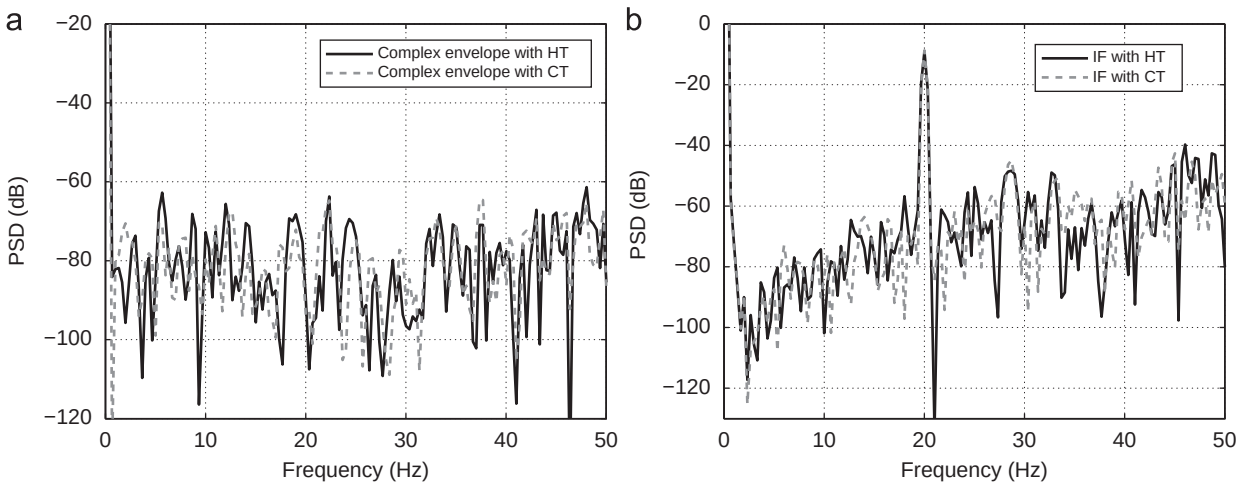

Fig. 3. Spectrum of IA and IF computed through the HT and CT in case of slow PM.

the contrary, CT requires only four multiplications and two additions and is instantaneous. For this reason CT should be preferred for slow and fast modulation cases.

4.2. Analysis of synthetic and real signals

4.2.1. Slow PM

Theoretically, there is no difference between the HT analytic signal and the CT space vector resulting from the CT in case of slow modulation.

Synthetic signals: The three fault currents submitted to PM are simulated according to the stator current model in (1) with an additive white Gaussian noise. The parameters are $I = 10$, $\alpha = 0$, $\beta = 0.03$, $\phi_{pm} = \pi/7$, $f_{pm} = 20\,\text{Hz}$, $f_s = 50\,\text{Hz}$, $\psi_0 = 0$ and the signal to noise ratio is $SNR = 37\,\text{dB}$. Fig. 3(a) and (b) shows, respectively, the spectrum of the simulated current IA and IF estimated by the HT and CT.

As expected in the case of a PM, a fault harmonic appears in the IF spectrum whereas the IA spectrum remains flat. The HT and CT lead to similar results. Table 1 indicates that the two transforms are also similar in case of slow AM.

Experimental signals: The experimental test bench is composed of a 5.5 kW, two pole pair induction machine supplied by a variable frequency Pulse Width Modulation inverter. The induction machine is coupled to a DC machine used as a mechanical load. The DC machine is connected to a resistor through a DC/DC converter which controls the DC motor armature current. The reference of the DC current is composed of an oscillating component at adjustable frequency plus an offset in order to induce load torque oscillations around a mean torque value. First consider experimental current measurements under load torque oscillations with $f_{pm} = 21\,\text{Hz}$ and $f_s = 50\,\text{Hz}$. According to the stator current model (4), the major modulation is a PM at frequency f_{pm}. The stator current spectrum shows fault signatures around the fundamental frequency, i.e. an increasing amplitude of the peaks at $f_s \pm f_{pm}$ (Fig. 4(a)). Distinction between PM and AM cannot be easily

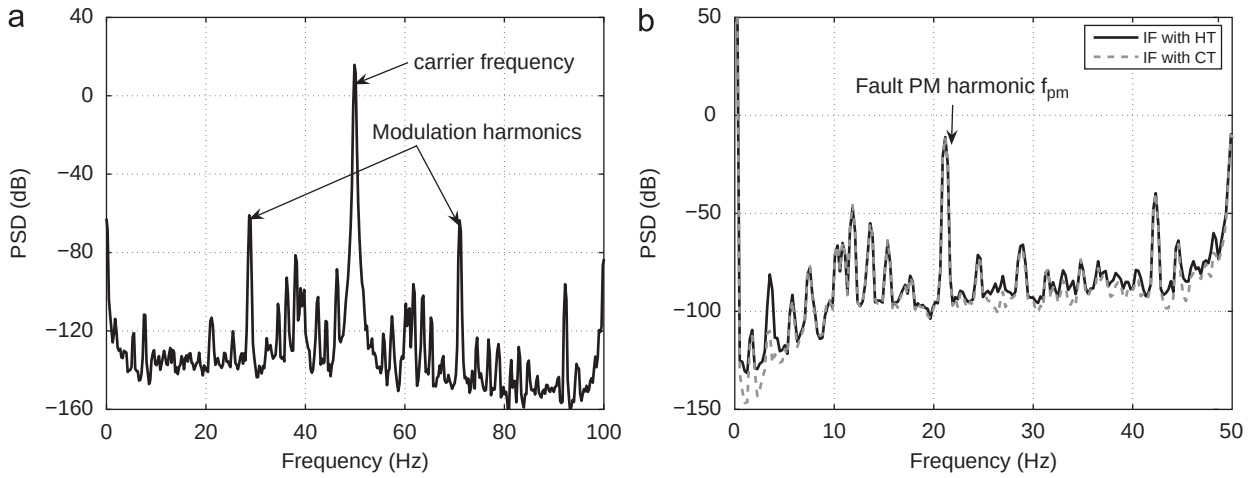

Fig. 4. Spectrum of stator current and associated IF computed through the HT and CT in case of slow PM.

performed using the spectrum. A separate analysis of the IA and IF is preferred (Fig. 4(b)). For slow modulated signals, the IF estimated with the HT and CT are similar.

4.2.2. Fast modulations

Synthetic signals: A stator current submitted to PM is simulated with the same model parameters, except for $f_{pm} = 70$ Hz, which is now larger than f_s. Fig. 5(a) and (b) shows, respectively, the spectrum of the IA and IF of the simulated current derived with the HT and CT.

As Bedrosian theorem hypothesis are not valid, the HT leads to extra harmonics at f_{pm} and $|2f_s - f_{pm}|$ frequencies on the IA spectrum, in accordance with Table 1. The CT leads to a unique harmonic at frequency f_{pm} on the IF spectrum and thus clearly reveals a fast PM. It can be noticed that similar results can be observed in case of fast AM according to Table 1.

Experimental signals: Experimental measurements are performed in case of load torque oscillations such as $f_{pm} \approx 81\,\text{Hz} > f_s$. As for simulated signals, the estimated IF with the HT creates an extra harmonic at $|2f_s - f_{pm}|$ frequency (Fig. 6(a)). The CT provides a unique harmonic related to the PM at f_{pm} frequency (Fig. 6(b)) and thus reveals that the major modulation is a PM at f_{pm} frequency.

5. Application to time-frequency diagnosis through Wigner distribution

5.1. Definition

The WD is a time-frequency energy distribution. The WD $W_z(t,v)$ of a complex signal $z(t)$ is defined as

$$W_z(t,f) = \int_{-\infty}^{\infty} z\left(t+\frac{\tau}{2}\right) z^*\left(t-\frac{\tau}{2}\right) e^{j2\pi f\tau}\, d\tau \tag{10}$$

where z^* denotes the conjugate of z. The WD is the FT of the kernel $K_z(t,\tau)$ with respect to the delay variable τ:

$$K_z(t,\tau) = z\left(t+\frac{\tau}{2}\right) z^*\left(t-\frac{\tau}{2}\right) \tag{11}$$

The WD is of strong interest for detection and diagnosis purposes in electrical drives, either in steady state or at variable speed. Indeed, unlike IA and IF spectra, the WD can be used in a non-stationary context i.e. at variable speed or variable carrier frequency. WD can also be used to detect the fault emergence in steady and transient state. Moreover, in steady and transient state operation, AM and PM (i.e. time-varying air-gap length and load torque oscillations) can be distinguished from the phase analysis of the WD interference structure [1,4].

First the WD expression has to be recalled in case of slow PM and AM.

5.2. Wigner distribution of steady state PM and AM currents

A pure slow PM can considered, with $\phi_0 = \phi_{pm} = 0$ to simplify. In this case, the HT and CT complex signals are equal such as

$$i_{CT}(t) = i_{HT}(t) = Ie^{j2\pi f_s t + \beta \sin(2\pi f_{pm} t)} \tag{12}$$

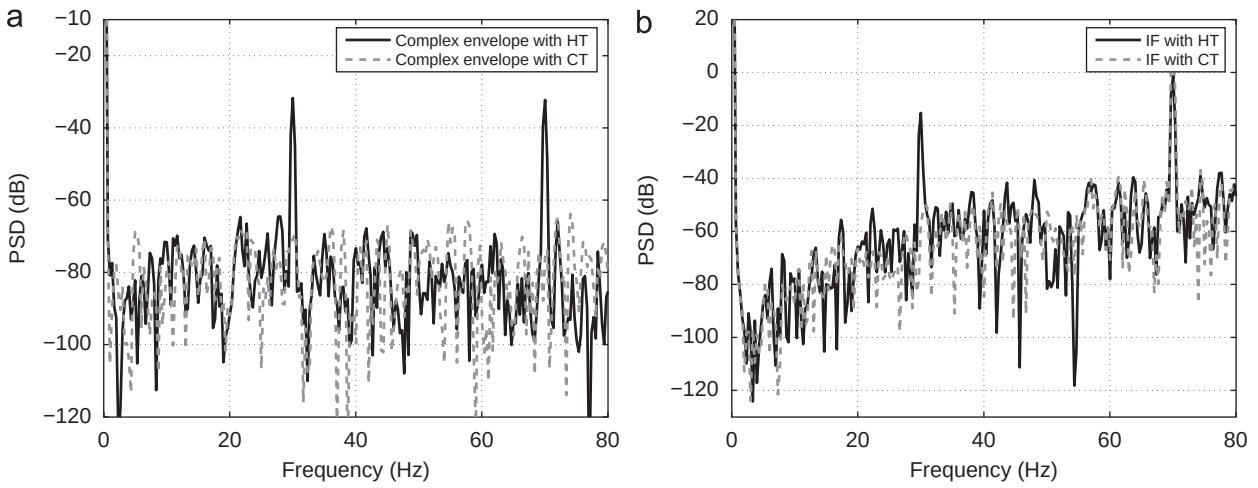

Fig. 5. Spectrum of simulated complex envelope and instantaneous frequency computed through the HT and CT in case of fast PM.

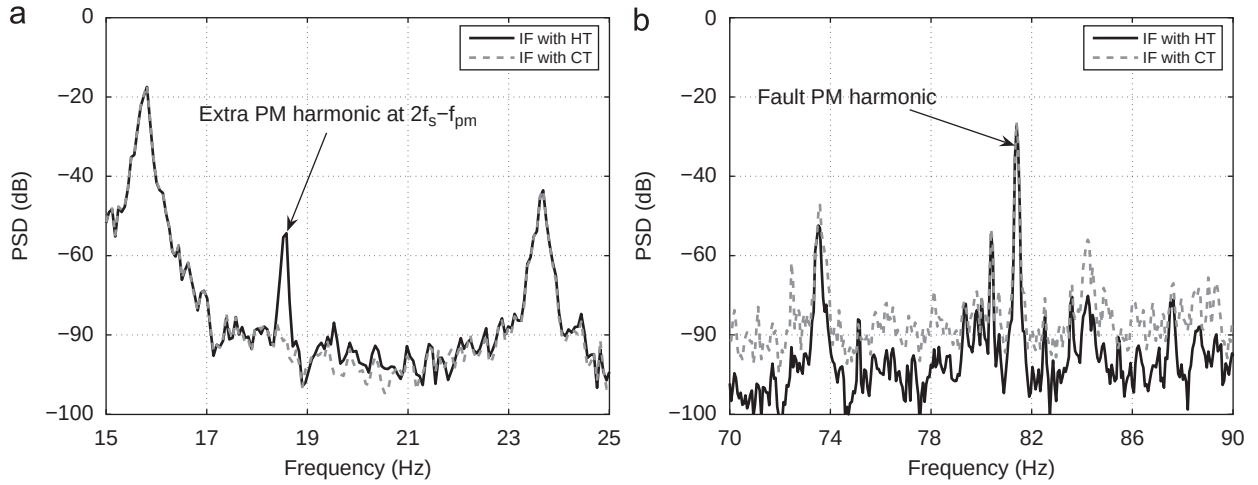

Fig. 6. Spectrum of IF computed through the HT and CT in case of fast PM.

The associated WD can be derived using the Jacobi–Anger expansion [4,23]:

$$W_{i_{HT}}(t,f) = W_{i_{CT}}(t,f) = I^2\delta(f-f_s) * \left[\sum_{n=-\infty}^{+\infty} J_n(2\beta\cos(2\pi f_{pm}t))\delta\left(f - n\frac{f_{pm}}{2}\right)\right] \quad (13)$$

where $J_k(\beta)$ denotes the k-th order Bessel function of the first kind. Now, a low level fault characterized by $\beta \ll 1$ is considered. According to Bessel function properties, $J_0(\beta) \simeq 1$ and $J_1(\beta) = -J_{-1}(\beta) \simeq \beta/2$ and higher order Bessel function terms may be neglected. The WD can be simplified in

$$W_{i_{HT}}(t,f) = W_{i_{CT}}(t,f) \simeq I^2\delta(f-f_s) + I^2\beta\cos(2\pi f_{pm}t)\left[\delta\left(f - f_s - \frac{f_{pm}}{2}\right) - \delta\left(f - f_s + \frac{f_{pm}}{2}\right)\right] \quad (14)$$

Thus the slow PM current WD is characterized by a fundamental component at f_s and periodic sidebands at $f_s \pm f_{pm}/2$ with frequency f_{pm}. Note that in case of PM, the sidebands are in phase opposition or with opposite signs.

Now, one can consider a pure slow AM signal with $\phi_0 = \phi_{am} = 0$ to simplify. The HT and CT are such as

$$i_{HT}(t) = i_{CT}(t)I[1 + \alpha\cos(2\pi f_{am}t)]e^{j2\pi f_s t} \quad (15)$$

A low level fault such as $\alpha \ll e1$ is considered. Straightforward derivations lead to the approached WD:

$$W_{i_{HT}}(t,f) = W_{i_{CT}}(t,f) \simeq I^2\delta(f-f_s) + I^2\alpha\cos(2\pi f_{am}t)\left[\delta\left(f - f_s - \frac{f_{am}}{2}\right) + \delta\left(f - f_s + \frac{f_{am}}{2}\right)\right] \quad (16)$$

The slow AM WD is characterized by a fundamental component and periodic sidebands at frequencies $f_s \pm f_{am}/2$ corresponding to the WD interference structure. It can be noticed that these components are periodic with frequency f_{am} and are in phase [1]. The phase shift (or the sign as an equivalent) of the sidebands can be used to distinguish slow AM and PM. According to Section 4, in the case of fast PM and AM, this diagnosis method remains valid when performed from the CT space vector. On the contrary HT leads to a misleading diagnosis in case of pure fast AM or PM. Indeed, both pure modulations appear as mixed AM and PM modulation according to Table 1. For instance, in the case of fast PM, the HT leads to an asymmetric interference structure with components at frequencies $f_s + f_{pm}/2$ and $f_{pm}/2$ and respective oscillating frequencies f_{pm} and $|2f_s - f_{pm}|$, as shown in Appendix A. The proposed diagnosis strategy cannot be applied.

Experimental stator currents have been measured on the machine in two steady state conditions, where the supply frequency equals $f_s = 13.3$ Hz and then $f_s = 50$ Hz with a load torque oscillation of frequency $f_{pm} \simeq 20$ Hz. Thus, the stator currents are fast and then slow PM signals. In Fig. 7(a), the WD is obtained through the HT analytic signal. In Fig. 7(b), the WD is computed using the CT space vector. In the slow PM case, the two WD are similar with sideband components in phase opposition at frequencies $f_s \pm f_{pm}/2$. However, in the fast PM case, the WD derived from the HT analytic signals leads to sideband components at frequencies $f_s + f_{pm}/2$ and $f_{pm}/2$ oscillating at f_{pm} and $|2f_s - f_{pm}|$ frequencies, respectively. The WD derived from the CT space vector leads to sideband components at frequencies $f_s \pm f_{pm}/2$ in phase opposition. Consequently, as previously demonstrated, the CT allows to detect the slow and fast PM in steady state conditions.

5.3. Wigner distribution of stator currents at variable speed

Finally, stator currents with variable supply frequency $f_s(t)$ and variable PM frequency $f_{pm}(t)$ are considered. Theoretical derivations have been performed in the particular case of a linear variation [4]. In this paper, the variable speed is considered only through simulations. Fig. 8 displays the simulated PM stator current WD. The PM frequency equals $f_{pm}(t) = 1.4 f_s(t)$ which correspond to fast modulated signals. As for steady state conditions, the WD computed from the CT space vector leads to sideband components at $f_s(t) \pm f_{pm}(t)/2$ in phase opposition whatever f_s. However, the WD obtained through the HT analytic signal leads to sideband components at frequencies $f_s(t) + f_{pm}(t)/2$ and $f_{pm}(t)/2$. It can be noticed that the two WD are similar in variable speed applications for slow modulated signals.

6. Conclusion

Amplitude and phase modulation analysis through spectral or time-frequency methods involves a complex signal for an univocal phase and amplitude definition. This paper compares the complex signals obtained with the Hilbert and Concordia transforms in case of slow and fast amplitude and phase modulations. This comparison is first conducted theoretically and then through simulated and experimental signals. The application to the time-frequency diagnosis based on Wigner distribution is developed. The Concordia transform provides an appropriate signal representation in the slow and fast modulation cases. On the contrary, the Hilbert transform is limited by the Bedrosian theorem conditions to the analysis of slow modulations. Phase and amplitude modulations, resulting from load torque oscillations and dynamic eccentricity, can be detected and distinguished using the Wigner distribution of the complex signal. The Wigner distribution via Concordia transform provides a clear modulation diagnosis through the estimation of the phase shift

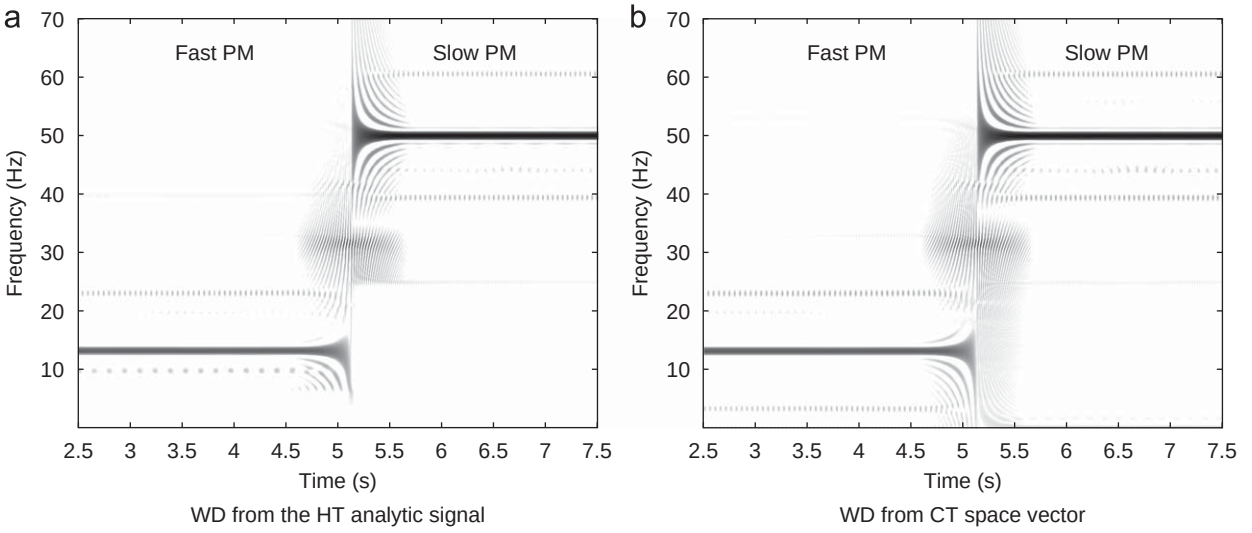

Fig. 7. WD computed using HT and CT for fast and slow PM experimental currents in steady state. (a) WD from the HT analytic signal. (b) WD from CT space vector.

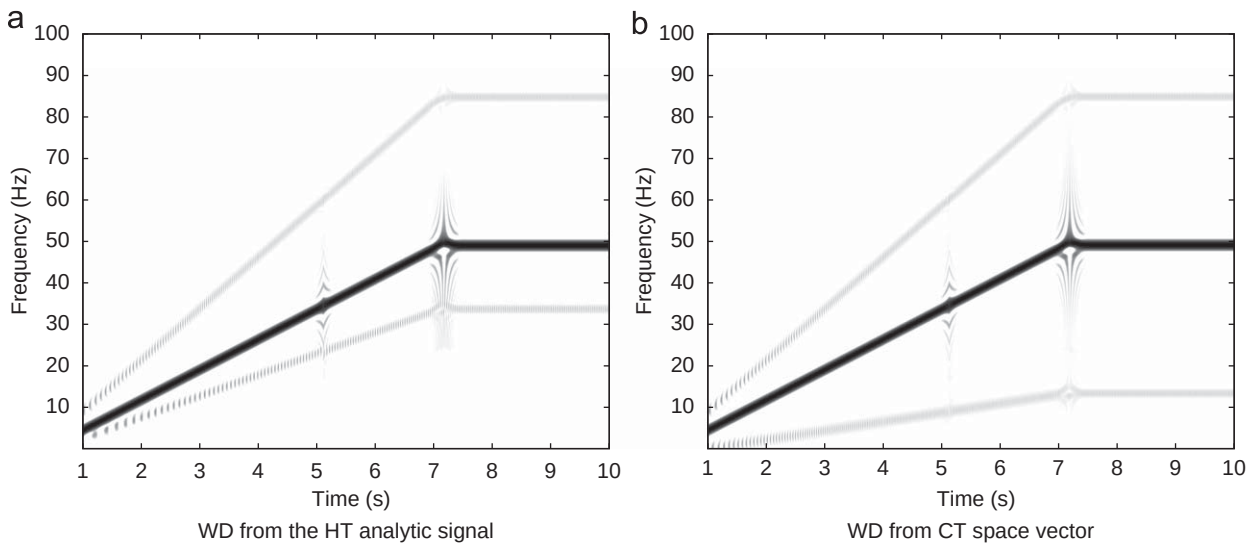

Fig. 8. WD from HT and CT for simulated fast PM at variable speed. (a) WD from the HT analytic signal. (b) WD from CT space vector.

between sideband components whatever the modulation frequency. Moreover, the Concordia transform is by far less expensive than the Hilbert transform in terms of computing complexity. As a consequence, when at least two stator current components are available, the Concordia transform should be preferred to build the complex signal required for the modulation analysis.

Appendix A. Fast PM stator current signal

One can consider the Hilbert transform of a PM stator current $i(t) = I\cos(2\pi f_s t + \beta\sin(2\pi f_{pm} t))$ according to the general model (1) with $\psi_0 = \phi_0 = \phi_{pm} = 0$. Assuming that $\beta \ll 1$, the FT can be approximated by

$$I(f) \simeq \frac{I}{2}[\delta(f-f_s)+\delta(f+f_s)] + \frac{I\beta}{4}[\delta(f-f_s-f_{pm})+\delta(f+f_s+f_{pm})] - \frac{I\beta}{4}[\delta(f-f_s+f_{pm})+\delta(f+f_s-f_{pm})] \tag{17}$$

Assuming that $f_s < f_{pm}$, the FT of the approximated analytic signal equals:

$$I_{HT}(f) = I\left[\delta(f-f_s) + \frac{\beta}{2}[\delta(f-f_s-f_{pm}) - \delta(f+f_s-f_{pm})]\right] \tag{18}$$

Thus, $i_{HT}(t)$ expresses as

$$i_{HT}(t) = Ie^{j2\pi f_s t} + I\beta\sin(2\pi f_s t)e^{j(2\pi f_{pm} t+\pi/2)} \tag{19}$$

In order to study the IA and IP, $i_{HT}(t)$ has to be expressed as $i_{HT}(t) = a_{HT}(t)e^{j\psi_{HT}(t)}$. The IA and IP, $a_{HT}(t)$ and $\psi_{HT}(t)$ are given by

$$\begin{cases} a_{HT}(t) = I\sqrt{1+\beta^2\sin^2(2\pi f_s t) + 2\beta\sin(2\pi f_s t)\sin(2\pi(f_s - f_{pm})t)} \\ \psi_{HT}(t) = 2\pi f_s t + \arctan\left[\dfrac{\beta\sin(2\pi f_s t)\cos(2\pi(f_{pm}-f_s)t)}{1-\beta\sin(2\pi f_s t)\sin(2\pi(f_{pm}-f_s)t)}\right] \end{cases} \tag{20}$$

Since $\beta \ll 1$, terms proportional to β^2 are neglected in the first order Taylor development of the square root leading to

$$a_{HT}(t) \simeq I\left[1 + \frac{\beta}{2}\left(\cos(2\pi f_{pm} t) - \cos\left(2\pi(2f_s - f_{pm})t\right)\right)\right] \tag{21}$$

Consequently, in case of fast PM, the Hilbert analytic signal IA shows two harmonics at f_{pm} and $|2f_s - f_{pm}|$ frequencies. These harmonics do not exist in case of slow PM. It can be noticed that there is no harmonic in the Concordia space vector IA, whatever the fundamental and the modulation frequencies.

With the same hypothesis on β, the approximated IP expresses as

$$\psi_{HT}(t) \simeq 2\pi f_s t + \left[\frac{\beta\sin(2\pi f_s t)\cos(2\pi(f_{pm}-f_s)t)}{1-\beta\sin(2\pi f_s t)\sin(2\pi(f_{pm}-f_s)t)}\right] \tag{22}$$

From first order Taylor development of the denominator and by neglecting terms proportional to β^2, the approximated IP expresses as

$$\psi_z(t) \simeq 2\pi f_s t + \frac{\beta}{2}\sin(2\pi f_{pm} t) + \frac{\beta}{2}\sin(2\pi(2f_s - f_{pm})t) \tag{23}$$

According to the definition in (7), the IF is given by

$$IF(t) \simeq f_s + \frac{\beta f_{pm}}{2}\cos(2\pi f_{pm} t) + \frac{\beta(2f_s - f_{pm})}{2}\cos(2\pi(2f_s - f_{pm})t) \tag{24}$$

Finally, in case of fast PM, the Hilbert analytic signal IF shows two harmonics at f_{pm} and $|2f_s - f_{pm}|$ frequencies. The harmonic at $|2f_s - f_{pm}|$ frequency does not exist in case of slow PM. The Concordia space vector IF has no extra harmonic whatever the fundamental and the modulation frequencies.

To obtain the WD signature of $i(t)$ using the HT, the kernel is expressed:

$$K_{i_{HT}}(t,\tau) = I^2 e^{j2\pi f_s \tau} + I^2\beta\cos(2\pi f_{pm} t)e^{j2\pi(f_s + f_{pm}/2)\tau} - I^2\beta\cos(2\pi(2f_s - f_{pm})t)e^{j2\pi(f_{pm}/2)\tau} \tag{25}$$

Then, the WD is derived:

$$W_{i_{HT}}(t,f) = I^2\delta(\nu - f_s) + I^2\beta\cos(2\pi f_{pm} t)\delta\left(\nu - f_s - \frac{f_{pm}}{2}\right) - I^2\beta\cos(2\pi(2f_s - f_{pm})t)\delta\left(\nu - \frac{f_{pm}}{2}\right) \tag{26}$$

References

[1] M. Blodt, J. Regnier, J. Faucher, Distinguishing load torque oscillations and eccentricity faults in induction motors using stator current Wigner distributions, in: Industry Applications Conference, vol. 3, October 2006, pp. 1549–1556.
[2] W.T. Thomson, On-line current monitoring to detect electrical and mechanical faults in three-phase induction motor drives, in: Proceedings International Conference on Life Management of Power Plants, December 1994, pp. 66–73.
[3] M. Blodt, M. Chabert, J. Regnier, J. Faucher, Mechanical load fault detection in induction motors by stator current time-frequency analysis, IEEE Transactions on Industry Applications 42 (6) (2006) 1454–1463.
[4] M. Blodt, D. Bonacci, J. Regnier, M. Chabert, J. Faucher, On-line monitoring of mechanical faults in variable-speed induction motor drives using the Wigner distribution, IEEE Transactions on Industrial Electronics 55 (2) (2008) 522–533.
[5] B. Boashash, Estimating and interpreting the instantaneous frequency of a signal—part 1: fundamentals, in: Proceedings of the IEEE, vol. 80, no. 4, April 1992, pp. 520–538.
[6] B. Boashash, Estimating and interpreting the instantaneous frequency of a signal—part 2: algorithms and applications, in: Proceedings of the IEEE, vol. 80, no. 4, April 1992, pp. 540–568.
[7] P. Flandrin, Time-Frequency/Time-Scale Analysis, Academic Press, San Diego, 1999.
[8] B. Picinbono, On instantaneous amplitude and phase signal, IEEE Transactions on Signal Processing 45 (3) (1997) 552–560.
[9] E. Bedrosian, A product theorem for Hilbert transforms, in: Proceedings of the IEEE, vol. 51, no. 5, May 1963, pp. 868–869.
[10] B. Trajin, J. Regnier, J. Faucher, Bearing fault indicator in induction machine using stator current spectral analysis, in: Power Electronics Machine and Drives Conference, April 2008, pp. 592–596.
[11] P. Vas, Electrical Machines and Drives—A Space-vector Theory Approach, Oxford Science Publications, Oxford, 1992.
[12] D.C. White, H.H. Woodson, Electromechanical Energy Conversion, Wiley, New York, 1959.
[13] A.J.M. Cardoso, A.M.S. Mendes, Converter fault diagnosis in variable speed DC drives, by Park's vector approach, in: Proceedings of the IEEE International Symposium on Industrial Electronics (ISIE'97), vol. 2, July 1997, pp. 497–500.
[14] V. Ignatova, P. Granjon, S. Bacha, F. Dumas, Classification and characterization of three phase voltage dips by space vector methodology, in: International Conference on Future Power System (FPS 2005), November 2005, pp. 1–6.
[15] S.M.A. Cruz, A.J.M. Cardoso, Stator winding fault diagnosis in three-phase synchronous and asynchronous motors, by the extended Park's vector approach, IEEE Transactions on Industry Applications 37 (5) (2001) 1227–1233.
[16] G.G. Acosta, C.J. Verucchi, E.R. Gelso, A current monitoring system for diagnosing electrical failures in induction motors, Mechanical Systems and Signal Processing 20 (4) (2000) 953–965.
[17] A.J.M. Cardoso, E.S. Saraiva, Computer aided detection of airgap eccentricity in operating three-phase induction motors, by Park's vector approach, in: IEEE Industry Applications Society Annual Meeting, September–October 1991, pp. 94–98.
[18] J. Zarei, J. Poshtan, An advanced Park's vectors approach for bearing fault detection, in: IEEE International Conference on Industrial Technology (ICIT'06), December 2006, pp. 1472–1479.
[19] J.L.H. Silva, A.J.M. Cardoso, Bearing failures diagnosis in three-phase induction motors by extended Park's vector approach, in: 31st Annual Conference of IEEE Industrial Electronics Society (IECON'05), November 2005, pp. 2591–2596.
[20] J.M. Aller, A. Bueno, T. Paga, Power system analysis using space-vector transformation, IEEE Transactions on Power Systems 17 (4) (2002) 957–965.
[21] J.R. Cameron, W.T. Thomson, Vibration and current monitoring for detecting airgap eccentricities in large induction motors, IEE Proceedings 133 (3) (1986) 155–163.
[22] D.G. Dorrell, W.T. Thomson, S. Roach, Analysis of airgap flux, current, and vibration signals as a function of the combination of static and dynamic airgap eccentricity in 3-phase induction motors, IEEE Transactions on Industry Applications 33 (1) (1997) 24–34.
[23] M. Abramowitz, I.A. Stegun, Handbook of Mathematical Functions with Formulas, Graphs, and Mathematical Tables, ninth ed., Dover Publications, New York, 1964.